Colloidal glasses and gels: The interplay of bonding and caging

Emanuela Zaccarelli[a] and Wilson C. K. Poon[b,1]

[a]Dipartimento di Fisica and Consiglio Nazionale delle Richerche–Istituto Nazionale per la Fisica della Materia–Soft: Complex Dynamics in Structured Systems, Università di Roma La Sapienza, Piazzale Aldo Moro 2, I-00185 Rome, Italy; and [b]Scottish Universities Physics Alliance (SUPA), and School of Physics and Astronomy, University of Edinburgh, Kings Buildings, Mayfield Road, Edinburgh EH9 3JZ, Scotland, United Kingdom

Edited by Hans C. Andersen, Stanford University, Stanford, CA, and approved July 16, 2009 (received for review March 2, 2009)

We report simulations of glassy arrest in hard-core particles with short-range interparticle attraction. Previous experiments, theory, and simulations suggest that in this kind of system, two qualitatively distinct kinds of glasses exist, dominated respectively by repulsion and attraction. It is thought that in the former, particles are trapped ''topologically,'' by nearest-neighbor cages, whereas in the latter, nonergodicity is due to interparticle ''bonds.'' Subsequent experiments and simulations have suggested that bond breaking destabilizes attractive glasses, but the long-term fate of these arrested states remains unknown. By running simulations to times a few orders of magnitude longer than those reached by previous experiments or simulations, we show that arrest in an attractive glass is, in the long run, also topological. Nevertheless, it is still possible to distinguish between ''nonbonded'' and ''bonded'' repulsive glassy states. We study the melting of bonded repulsive glasses into a hitherto unknown ''dense gel'' state, which is distinct from dense, ergodic fluids. We propose a ''modified state diagram'' for concentrated attractive particles, and discuss the relevance of our results in the light of recent rheological measurements in colloid–polymer mixtures.

colloids | glass transition | nonergodicity

Understanding glassy arrest is one of the ''grand challenges'' facing 21st century condensed-matter science. In this endeavor, the study of well-characterized ''model'' systems, whether by simulations or experiments, plays a unique role. Although such systems are often quite far removed from real-world materials applications, their study can generate clear-cut data against which theories can be tested directly. A paradigmatic example of such synergism is provided by the investigation of glass transitions in systems of repulsive particles with short-range interparticle attraction at high particle concentrations (Fig. 1). Mode-coupling theory (MCT) predicts that in such a system, two qualitatively distinct arrested states should exist (1–4): a repulsion-dominated glass in which nonergodicity is due to the topological trapping of particles by each other in ''cages,'' and an attraction-dominated glass in which particles are trapped by nearest-neighbor ''bonds.'' These predictions were subsequently confirmed by experiments using well-characterized model colloids in which a short-range interparticle attraction was induced by nonadsorbing polymer via the ''depletion'' effect (5, 6). Simulations similarly verified this picture (7–10). The large measure of agreement between results obtained from the three methodologies is striking. MCT can, for example, account semiquantitatively for the experimental glass transition boundaries in colloid–polymer mixtures (11) and predict aspects of the functional form of density–density correlation functions measured in dynamic light-scattering measurements (12).

Nevertheless, significant qualitative disagreements were evident from the beginning, especially in the long-time behavior of attractive glasses. A key quantity is the intermediate scattering function, $f(q,t)$, which measures the decay with time (t) of density fluctuations at length scale $\approx 2\pi/q$ (where q is the magnitude of the scattering vector). The MCT glass transition involves an abrupt change of the nonergodicity parameter $f(q,\infty)$ from zero to some (q-dependent) finite value, f_q. MCT predicts that upon moving from repulsive to attractive glass across the glass–glass transition line (Fig. 1), there should be a step increase in the value of f_q (3), reflecting the higher degree of confinement in interparticle bonds than in a topological cage. The decay of $f(q,t)$ to a constant, finite value at long times has long been seen in simulated hard spheres (HS) and experimental measurements in HS-like colloids, with MCT well predicting the value of the nonergodicity parameter as a function of both q and particle concentration (13, 14). However, first results from experiments (5, 6) on attractive glasses did not show such ''decay to a plateau'' in $f(q,t)$. Rather, the typical attractive glass $f(q,t)$ first decays to a high value consistent with nonergodicity parameter predictions by MCT, where it shows a point of inflection, and then continues to decay noticeably (but by no means completely) within the experimental time window.

More extensive experiments (12) as well as simulations (15) subsequently confirmed this picture, with the latter showing convincingly that this is not an artifact due to aging. Authors of the simulation work proposed that such decay was due to bond-breaking processes, but suggested that studying the long-term fate of attractive glasses was perhaps ''beyond computational efforts'' (16). Here, we perform simulations over more than eight orders of magnitudes in time, some three orders longer than in previous work, and show that arrest in an attractive glass is, in the long run, also attributable to trapping by topological cages. Nevertheless, it still appears possible to distinguish between the states hitherto known as repulsive and attractive glasses, which we propose to rename ''nonbonded'' and ''bonded' repulsive glasses, respectively.

Another unresolved issue in the study of arrest in ''sticky-particle'' systems is how attractive glasses relate to gels (1, 11, 17–19). Traditionally, the term ''gel'' is used in materials science to refer to a system that behaves like a soft solid (i.e., has a finite shear modulus in the low frequency limit) that nevertheless contains a very large amount (say, much more than 50%) of liquid. It is well known that colloids with strong enough interparticle attraction can form gels (reviewed in ref. 20), with particle volume fraction (ϕ) as low as $\approx 10^{-2}$. It is by now well established that in systems of spherical particles with isotropic short-range attraction at $\phi \lesssim 0.4$, gelation is often the result of arrested spinodal decomposition (21). (The evidence is reviewed in ref. 17.) But the status of the arrested states in attractive particle systems at higher particle concentrations ($\phi \gtrsim 0.4$), and whether these states are distinguishable from the attractive glasses predicted by MCT, remains unclear.

Our simulations show that the ''bonded repulsive glass'' melts into a previously undescribed state as the packing fraction is

Author contributions: E.Z. and W.C.K.P. designed research; E.Z. performed research; E.Z. analyzed data; and E.Z. and W.C.K.P. wrote the paper.

The authors declare no conflict of interest.

This article is a PNAS Direct Submission.

[1]To whom correspondence should be addressed. E-mail: w.poon@ed.ac.uk.

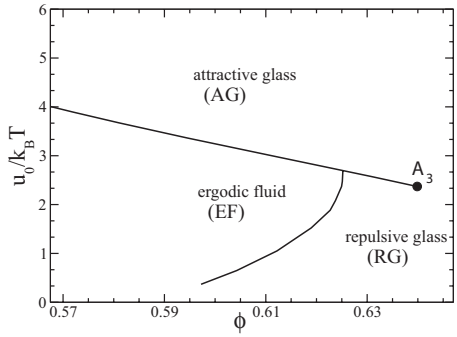

Fig. 1. Currently accepted state diagram of hard spheres with short-range square-well attraction (depth u_0 normalized to the thermal energy, k_BT) at high volume fraction (ϕ), showing three distinct states: ergodic fluid (EF), repulsive glass (RG) and attractive glass (AG). The distinction between RG and AG ends at the so-called A_3 point. The boundaries shown have been previously determined (24) for the same system of ''sticky bidisperse hard spheres'' as investigated in this work (see *Materials and Methods* for details).

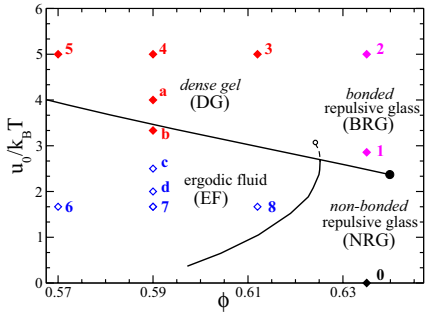

Fig. 2. Samples simulated in this work (labeled points) superimposed on the state diagram previously determined (24) for our system of sticky bidisperse hard spheres (continuous lines; axes as in Fig. 1). Our simulations show that four distinct states exist: ergodic fluid (EF), nonbonded repulsive glass (NRG), bonded repulsive glass (BRG), and dense gel (DG). The ''metastable continuation'' of the boundary between EF and NRG is shown (dashed) and terminates at an end point (open circle).

lowered. We argue that this state can appropriately be named a ''dense gel,'' and that there is indeed an in-principle well-defined distinction between what until now were known as attractive glasses and these gels.

Taken together, our results give rise to a ''state diagram'' for dense systems of hard particles with short-range attraction, consisting of four distinct states: nonbonded and bonded-repulsive glasses, dense gels, and ergodic liquid. Recent rheological experiments (22, 23) support this picture, but there is no theory to date that can account for the existence and properties of all four states.

Results

We studied a binary mixture of 700 hard spheres with a short range (3% × particle diameter) attraction via event-driven molecular dynamics (MD) simulations (see *Materials and Methods* for details). The behavior of this system is controlled by the depth of the square-well attraction, u_0, relative to the thermal energy, k_BT, and the particle volume fraction, ϕ. The state diagram of this system in the (ϕ, u_0/k_BT) plane has been established previously by both MCT calculations and simulations (24) (Fig. 1). We calculated the time-dependent single-particle mean squared displacement (MSD), $\langle \Delta r^2(t) \rangle$, over eight or more decades of time, $10^{-2} \lesssim t < 10^6$ (with time in MD units, see *Materials and Methods*), which is three orders of magnitude greater than the longest times reached in previous simulations or colloidal experiments. All data in the nonergodic region correspond to a waiting time $t_w \simeq 10^7$, providing waiting-time-independent data up to $t \approx 10^6$. Our results for three sequences of samples through state space, Fig. 2, are shown in Figs. 3–5.

Consider first the sequence of samples 0 to 5, Fig. 3. Sample 0 is a hard-sphere glass at $\phi = 0.635$, where particles ''cage'' each other topologically. After free motion at the shortest times accessed ($t \lesssim 2 \times 10^{-2}$), the MSD turns over and saturates to a plateau, $\langle \Delta r^2 \rangle \approx 4 \times 10^{-3}$ (in units of the squared particle diameter), at later times, $t \gtrsim 10^{-1}$, and stays at this value to the longest times accessed in our simulations.

After more or less free motion at the shortest times, particles in sample 1 are trapped briefly at an MSD of $\langle \Delta r^2 \rangle \approx 6 \times 10^{-4}$. Soon, however, the MSD starts to increase again, until it saturates at the HS plateau of sample 0.

The significantly slower dynamics in sample 2 led to noisier data at the longest times. We show five separate realizations of the MSD (whereas data previously shown for samples 0 and 1 were averaged over the same number of realizations). The noise at long times is clear, but the same trend as sample 1 is also evident. Particles are briefly delayed at $\langle \Delta r^2 \rangle \approx 4 \times 10^{-4}$, and their subsequent subdiffusive average motion appears bounded by the HS cage value of $\langle \Delta r^2 \rangle \approx 4 \times 10^{-3}$.

There is little qualitative difference between the MSD of sample 3 and samples 1 and 2 at short and medium times. At $t \gtrsim 10^3$, however, a qualitative difference does emerge. The MSD for sample 3 does not saturate, but increases subdiffusively (i.e., $\langle \Delta r^2(t) \rangle \propto t^\alpha$ with $0 < \alpha < 1$) to the longest times studied. This long-time subdiffusive motion becomes faster (i.e., larger α) as ϕ is further lowered (samples 4 and 5).

Turning to samples 6–8 (Fig. 4), we see that they are ergodic fluids. The MSD of sample 6 shows a point of inflection and incipient plateau at $\langle \Delta r^2 \rangle \approx 2 \times 10^{-2}$, between short-time ballistic and long-time diffusive behavior. Increasing ϕ but keeping u_0 constant, we observe that the point of inflection moves to longer times, and the width of the incipient plateau increases. Nevertheless, all three samples retain diffusive behavior at long times.

Discussion

The results shown in Figs. 3 and 4 up to $t \gtrsim 10^3$ are consistent with findings from previous simulations of the same system (15,

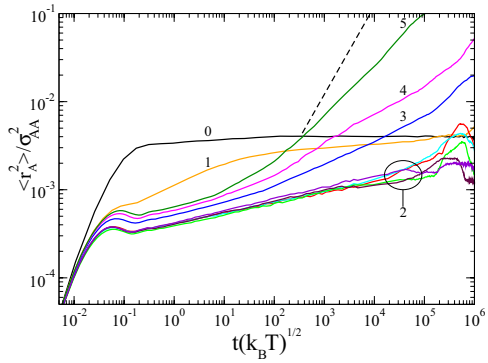

Fig. 3. Calculated mean-squared displacement (MSD), $\langle \Delta r^2 \rangle$, of samples 0–5 (Fig. 2) normalized by the squared diameter of the larger particles versus time, $t(k_BT)^{1/2}$, where the temperature factor normalizes the contributions of different thermal velocities. In all cases except sample 2, the results have been averaged over at least 5 independent runs, whereas 5 independent runs are shown for sample 2. Sample 1 is a bonded repulsive glass, with the MSD saturating at the (squared) cage size. Sample 2 is a bonded repulsive glass; its MSD shows a transient plateau due to interparticle bonds before saturating at the squared cage size. Samples 3–5 are dense gels; their MSDs again show a transient plateau due to interparticle bonds but then do not saturate again thereafter. The dashed line has unit slope.

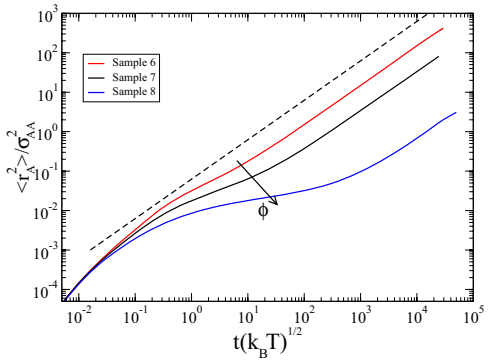

Fig. 4. Calculated mean squared displacement (MSD) of samples 6–8 (Fig. 2), which are ergodic fluids. Axes as in Fig. 3. The dashed line has unit slope.

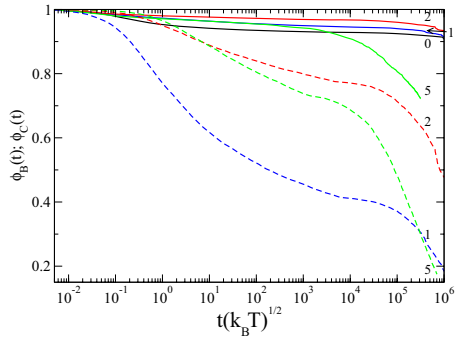

Fig. 6. Cage (solid lines) and bond (dashed lines) correlations functions, $\Phi_C(t)$ and $\Phi_B(t)$, plotted against time for samples 0 (nonbonded repulsive glass), 1, 2 (bonded repulsive glasses), and 5 (dense gel).

16, 24). Within the state diagram established by previous work (Fig. 1) sample 0 should be a repulsive glass and samples 1–5 should be attractive glasses, whereas sample 6–8 should be ergodic fluids. Extending the simulations by three orders of magnitude does not change our understanding of samples 0 and 6–8. The data obtained from the extra decades of time do, however, significantly alter our understanding of samples 1–5.

Bonded Repulsive Glass. Within the framework established by previous work (1–3, 5–10), samples 1 and 2 would be classified as attractive glasses. Their MSDs initially saturate at $\langle \Delta r^2 \rangle \approx 5 \times 10^{-4}$, which is the same order as the square of the width of the interparticle attraction (0.03^2), i.e., particles spend significant time trapped by nearest-neighbor attractive bonds.

However, as found previously, this "bond trapping" is not permanent. After displaying a transient plateau, the MSD continues to increase, and eventually saturates again at the HS value found for sample 0 (Fig. 3). This saturation is particularly clear in sample 1.

We interpret these findings as follows. At $t \lesssim 10^{-1}$, each particle is indeed trapped by bonds with a particular set of neighbors. These bonds start to break beyond this time scale (15, 16) while bonds reform with a different set of neighbors. After multiple breaking and reforming of such bonds, each particle finds itself still trapped topologically by its cage of neighbors.

Direct evidence for this interpretation comes from cage- and bond-correlation functions, $\Phi_C(t)$ and $\Phi_B(t)$, Fig. 6 (see *Materials and Methods* for details). The decay of $\Phi_C(t)$ [$\Phi_B(t)$] from unity signifies the replacement of topological (bonded) neighbors at time 0. Over the nearly nine decades we studied, there is little decay of $\Phi_C(t)$ for samples 0, 1, or 2, staying above 0.9 in all cases.

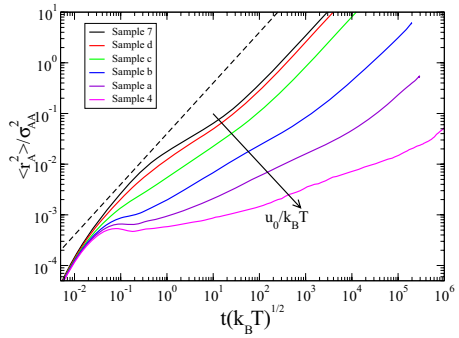

Fig. 5. Calculated MSD of samples 4, a, b, c, d, and 7 (Fig. 2). Axes are as in Fig. 3. Samples c, d, and 7 are ergodic fluids; these MSDs did not show waiting-time dependence. Samples 4, a, and b are dense gels; these MSDs were found to show aging. The straight line has unit slope.

However, in samples 1 and 2, where there are attractive bonds, their $\Phi_B(t)$ show significant decay in the same time window (to $\approx$0.2 and $\approx$0.6 respectively). The "glassiness" of these samples on the time scale we have studied is therefore not, ultimately, due to interparticle attraction; instead, like sample 0, topological caging dominates at long times. The nomenclature of "attractive glass," therefore, appears inappropriate.

But samples 1 and 2 are qualitatively distinguishable from sample 0: Their MSDs show distinct, transient plateaus at the length scale of interparticle bonds, a feature absent in repulsive glasses, such as our sample 0. We therefore propose the name "bonded repulsive glasses" (BRG) for the region of state space in which samples 1 and 2 are situated.

In this light, those states previously known as repulsive glasses (including our sample 0) should then be called "nonbonded repulsive glasses" (NRG): Here, the "topological plateau" in the MSD is reached in a single step, without going via an intermediate (transient) plateau due to bonding.

Dense Gel. Within the framework established by previous work (1–3, 5–10), samples 3–5 should also be attractive glasses. Indeed, up to the time scale of previous simulations ($t \gtrsim 10^3$), their behavior is qualitatively indistinguishable from samples 1 and 2: Their MSDs all show transient plateaus at $\langle \Delta r^2 \rangle \gtrsim 4 \times 10^{-4}$, evidencing the effect of interparticle bonds, and then subdiffusive motion at longer times due to bond breaking (15, 16). However, our simulations up to $t = 10^6$ support a different conclusion. The long-time-limit saturation at the interparticle cage seen in samples 1 and 2 is absent from samples 3–5. Instead, apparently unbounded (but subdiffusive) behavior is seen at long times.

Note that these samples are distinguishable from the ergodic fluid state. To reach this state starting from samples 3–5 (Fig. 4) we have to lower the interparticle attraction. We have done this for a sequence of samples (a,b,c,d) with $\phi = 0.59$ and u_0 intermediate between sample 4 ($u_0/T = 5$) and sample 7 ($u_0/T = 1.67$) (Fig. 5). As u_0 is lowered (samples 4, a, b), the subdiffusive exponent α for the long-time motion increases, until the long-time motion becomes diffusive ($\alpha = 1$) in samples c, d, and 7. Moreover, we observe that samples 4, a, and b show aging, while no waiting time dependence is observed for samples c, d, and 7. Thus, the latter three samples are clearly ergodic fluids. However, samples 4, a, b (together with 3 and 5) are neither ergodic fluids nor BRG. We propose to call samples 3, 4, 5, a, and b "dense gels" (DG), to distinguish them from BRG on the one hand and more dilute gels due to arrested spinodal decomposition (17) on the other. The latter distinction is supported by the observation that the structure factors (or, equivalently, real-space pair correlation functions) of these samples did not change

during aging (see ref. 16). Moreover, their structure factors do not show any increase at small wave vectors, as occurs in phase-separating systems (21, 25).

Once again, our interpretation is supported by calculated cage- and bond-correlation functions. Results for sample 5 are shown in Fig. 6. We see that there is significant bond as well as cage breaking, revealed as decay in both $\Phi_C(t)$ and $\Phi_B(t)$ over our simulation window. Not unexpectedly, bond breaking proceeds at a faster rate than cage breaking. Indeed, the decay in $\Phi_C(t)$ is far from complete over our time window. This suggests that as each particle moves, it "carries along" with it a remnant of its initial geometric cage, presumably because of the existence of interparticle attraction. In other words, over the time window simulated, each diffusing particle carries with it "memory" of its bonded neighbors. Memory is known to lead to subdiffusive behavior (26–29).

Transition Boundaries. Our simulations have found four distinct states in a system of attractive hard spheres at high concentrations: NRG, BRG, DG, and ergodic fluids. The length of the simulation runs needed to determine dynamical properties, especially of BRG samples, has limited the number of state points we were able to investigate. Future work studying many more samples will be needed to locate precisely the boundaries between these states. Nevertheless, previous simulations together with the result presented above already give important clues to the positions of various transition boundaries. In particular, although MCT only predicts three states in this system (ergodic fluid, repulsive, and attractive glasses) and its prediction of permanent trapping by bonds is untenable (ref. 24 and this work), it appears that the boundaries between the three different MCT states for our system (Fig. 1) still mark the transition between some of the states we have found.

First, MCT predicts that there is a discontinuous transition between repulsive glass and attractive glass at high ϕ. Previous simulations (24) have already revealed that such a transition occurred only if a repulsive barrier was added to the interparticle potential to prevent bond breaking. Without this barrier, the system dynamics evolved continuously and bond trapping is not permanent. Nevertheless, the MCT transition [suitably scaled (30)] between repulsive and attractive glasses (occurring at $T = 0.4$ at $\phi = 0.635$) was found to coincide with the point at which a transient plateau due to bonding first emerged in reciprocal space–density correlators (see the bottom panel of figure 2 in ref. 24). The real-space equivalent of this finding is that the MCT repulsive–attractive glass boundary is also where a transient plateau first emerges in real-space MSDs, i.e., the boundary between what we have called NRG and BRG.

Second, at lower ϕ, MCT predicts a discontinuous transition between ergodic fluid and attractive glass. There have been few previous studies of this transition (but see ref. 31). Our results for samples 4, a, b, c, d, and 7 (Figs. 2 and 5), show that the boundary predicted by MCT must be very close to the boundary between our DG and ergodic fluid.* Again, however, whereas MCT predicts a discontinuous transition, our simulations (Fig. 5) show that the change from ergodic fluid to DG is continuous.

Third, MCT is able to predict the boundary at which attraction melts the repulsive glass into an ergodic fluid (30). Our work does not change this conclusion, except that the repulsive glass has become our NRG.

The fourth and final issue is the boundary between BRG and DG. There is good qualitative reason to expect a clear transition between these two states, because the underlying physics is the same as that of the melting of NRG to ergodic fluid: If interparticle attraction is able to create enough "free volume" by clustering some of the particles, then permanent caging no longer obtains. Thus, one may surmise that the boundary between BRG and DG should be the extrapolation of the boundary between NRG and ergodic fluid. Visual inspection of Fig. 2 shows that this is indeed plausible.

If that is the case, then one could surmise that the metastable continuation of the MCT boundary between the repulsive glass and ergodic fluid may be related to the BRG–DG boundary. Such continuation can in fact be done by solving the MCT long-time-limit equations for the nonergodicity parameter (32) inside what previously is known as the attractive glass region, starting the iterative scheme from a repulsive glass solution (1). We have done this calculation (dashed line, Fig. 2). As found previously (1, 33), there is only a very small range of u_0/k_BT over which this "metastable continuation" exists: It terminates rather abruptly at an end point (open circle, Fig. 2).† De novo theoretical developments are necessary to predict this boundary properly.

Relation to Experiments. Direct experimental tests of what we propose here will probably come from particle tracking in the kind of well-characterized colloid–polymer mixtures that have been used before to study glassy states in sticky-particle systems (5). Such experiments will be challenging, because of both the long times involved and the high precisions needed. Recent advances in data analysis (34) mean that tracking to the precision needed (better than the range of the interparticle attraction) should now be possible. Successful measurement of MSDs to long time also requires the ability to remove rather precisely large-scale coherent motions due to stage drift and other extraneous sources; this is now also possible (35). These advances together should enable direct tests of our proposals. On the other hand, indirect experimental corroboration of our findings already exists in the form of recent rheological studies of model colloids (22, 23). Under oscillatory strain of increasing amplitudes, a nonbonded repulsive glass (simply "repulsive glass" in refs. 22 and 23) was found to yield in one step, at a strain amplitude consistent with the size of the nearest-neighbor cage. On the other hand, a bonded repulsive glass ("attractive glass" in refs. 22 and 23) was found to yield in two steps. Nonlinearity was observed to set in first at a strain amplitude corresponding to the range of nearest-neighbor bonds, but complete yielding was not observed until a strain amplitude sufficient to break cages was reached. This is consistent with our interpretation of the MSD of samples 1 and 2 (Fig. 3) and their respective cage and bond correlation functions (Fig. 6). Significantly, an attractive glass at lower volume fraction, corresponding to the dense gel in this work, was found to yield in a single step, corresponding to the breaking of nearest-neighbor bonds. Again, this is consistent with our interpretation of the lack of caging after bond breaking in dense gels (samples 3, 4, 5, a, and b).

Summary and Conclusions

A schematic way to summarize and make sense of our findings at the high-ϕ end of the state diagram (Fig. 2) is as follows. Increasing u_0/k_BT from zero, we encounter a boundary that runs essentially from left to right, which separates states in which the MSD shows no sign of time and length scales set by the interparticle attraction, from states in which the MSD does show

*The correspondence is not exact, because our sample b lies just below the position of the MCT line, but is a DG according to our simulations.

†A possible way to extend this line, beyond the end point, would be to continue solving the MCT equations, again starting the iterative scheme from a repulsive glass solution, even if we then find either an ergodic or an attractive solution. This procedure, however, has doubtful theoretical validity. Nevertheless, for completeness, we record that carrying out this calculation for our system produces a line that continues beyond the end point shown in Fig. 2 and passes approximately halfway between samples 3 and 4, whereas our simulations suggest that the BRG-DG boundary is probably between samples 2 and 3.

the influence of this attraction. On the other hand, decreasing ϕ (essentially from random close packing), we encounter a boundary that runs from bottom to top, which separates states in which the particle concentration is high enough to cage each other geometrically from states in which such caging no longer exists. The actual boundaries are neither strictly horizontal nor strictly vertical, reflecting the influence of density on attraction and vice versa. Nevertheless, this schematic picture captures the essential physics uncovered by our simulations, and shows why four qualitatively distinct regimes of behavior may be expected: bonded repulsive glass (attraction and cages both important), nonbonded repulsive glass (cages alone are important), dense gel (attraction alone is important), and ergodic fluid.

Indirect experimental evidence for the findings of our simulations comes from recent rheological studies (22, 23), showing a two-step yielding of BRG under oscillatory strain of increasing amplitude. Direct confirmation awaits high-precision measurements of MSD in, e.g., colloid–polymer mixtures, to long times. To date, no theory offers a quantitative account of the long-time behavior of the BRG and DG states revealed by our simulations, which involves "hopping processes" in the form of bond breaking (36). Finally, we mention that at time scales still longer than those probed here, hopping between cages may destroy even the NRG and BRG.

Materials and Methods

Simulations. We perform event-driven MD simulations for a binary mixture of particles (species *A* and *B*) interacting via a narrow square-well (SW) potential. This system was extensively studied previously by means of theory (MCT) and simulations (9, 24). The combination of both tools allowed us to determine, within the limits of certain well-defined approximations, the location of the ideal glass lines for this particular system (24).

The parameters of the mixture are chosen to avoid crystallization in the system. Thus, we consider a 50:50 mixture of 700 particles of mass m with diameters $\sigma_{AA} = 1.2$ and $\sigma_{BB} = 1$; the hard-core diameter for the *AB* interaction is $\sigma_{AB} = (\sigma_{AA}+\sigma_{BB})/2$. We fix the width of the attractive well as $\Delta_{ij}/(\sigma_{ij} + \Delta_{ij}) = 3\%$. Temperature is measured in units of the well depth u_0, whereas time units are $\sigma_{BB}(m/u_0)^{1/2}$. Within the ergodic region, configurations are directly equilibrated for the desired density and temperature. For dense gels, the system is at first equilibrated at the same density but a higher temperature and then quenched to the target temperature. For glassy state points, independent configurations were generated in the reentrant, ergodic region (specifically at $\phi = 0.612$ and $k_BT/u_0 = 0.6$) and rapidly compressed, in small steps, to the desired packing fraction. Then, an instantaneous quench was performed to the final temperature (15). The time of the quench is defined as the starting time. We checked for crystallization by computing structure factors and detected none.

Simulations are performed in the *NVT* ensemble, with a thermostat with a very short characteristic time keeping the temperature constant during the whole run. For ergodic state points, the thermostat is removed after the system has reached equilibrium and data are collected in the *NVE* ensemble.

When simulating state points within the glass region, i.e., in an out-of-equilibrium state, the properties of the system (e.g., correlation functions) depend not only the time of observation t but also on the time elapsed from the initial quench to the studied state point, the so-called waiting time t_w. For $t \ll t_w$, correlation functions for different t_w are found to collapse on the same curve—a phenomenon connected to the equilibration of the degrees of freedom faster than t_w (37). In this way, t_w-independent data can be generated. Therefore, in previous studies, the system was monitored only within a very short time window, limited to 400 MD units in ref. 15 and up to one more order of magnitude in ref. 16.

To investigate the long-time limit of the attractive glass, we have monitored the evolution of the system for a total time well above 10^7 units in all studied cases. This allows us to show a t_w-independent window of up to 10^6 MD units. Therefore, we have been able to extend our previous investigations by more than three orders of magnitude. The longest runs (e.g., sample 2) took up to 6 months on a 3-GHz Xeon processor. To average over different initial configurations, we considered for each state point at least five independent runs.

Data Analysis. The data analysis is performed in a standard way for ergodic state points (i.e., averaging independent configurations over time after equilibration), whereas the dependence on the waiting time is monitored for nonergodic state points. In particular, we have chosen to focus on the case $t_w = 1 \times 10^7$ MD units. This ensures that our results are independent of the choice of t_w for the subsequent 10^6 MD units. Data were averaged over the five independent configurations. To reduce numerical noise for the MSD, we have also averaged over time in a limited time window around t_w.

Cage and bond correlations functions, $\Phi_C(t)$ and $\Phi_B(t)$, are calculated as

$$\Phi_{C,B}(t) = \left\langle \sum_{i<j} n^{ij}_{C,B}(t_w) n^{ij}_{C,B}(t + t_w) \right\rangle / [N_{C,B}(t_w)],$$

where $n^{ij}_{C,B}(t)$ is 1 if particles i and j are, respectively, found within the cage or bond distance, and 0 otherwise. $N_{C,B}(t)$ is the total number of neighbors within the cage or bond distance at time t. The bond distance is defined unambiguously as the total range of the potential $\sigma_{ij} + \Delta_{ij}$, whereas the cage distance depends on ϕ, and it is defined as the length at which the MSD, calculated for the corresponding hard-sphere mixture at the same packing fraction, displays an inflection point.

MCT Calculations. The static structure factor to be used as input for MCT equations was determined by solving the Ornstein–Zernike equation for our SW binary mixture numerically. The MCT long-time-limit equations were solved iteratively by using a grid of 500 wave vectors with mesh 0.5. To determine the extension of the repulsive glass line inside the attractive glass region, we followed ref. 1 and used a repulsive solution for the nonergodicity parameters as initial guess for the calculations.

ACKNOWLEDGMENTS. We thank J. Bergenholtz for discussions; Mike Cates, Chantal Valeriani, and Rut Besseling for commenting on the manuscript; and the Edinburgh Computing and Data Facility for providing resources. This work was supported by Engineering and Physical Sciences Research Council Grants EP/D071070 and EP/E030173 (to W.C.K.P.). The collaboration was, in part, supported by European Union Grant NoE "SoftComp" NMP3-CT-2004-502235 and by the Marie Curie Network on Dynamical Arrest of Soft Matter and Colloids Grant MRTNCT-2003-504712.

1. Bergenholtz J, Fuchs M (1999) Nonergodicity transitions in colloidal suspensions with attractive interactions. *Phys Rev E* 59:5706–5715.
2. Fabbian L, Götze W, Sciortino F, Tartaglia P, Thiery F (1999) Ideal glass–glass transitions and logarithmic decay of correlations in a simple system. *Phys Rev E* 59:R1347–R1350.
3. Dawson K, et al. (2000) Higher-order glass-transition singularities in colloidal systems with attractive interactions. *Phys Rev E* 63:011401.
4. Sciortino F, Tartaglia P (2005) Glassy colloidal systems. *Adv Phys* 54:471–524.
5. Pham KN, et al. (2002) Multiple glassy states in a simple model system. *Science* 296:104–106.
6. Eckert T, Bartsch E (2002) Re-entrant glass transition in a colloid–polymer mixture with depletion attractions. *Phys Rev Lett* 89:125701.
7. Puertas AM, Fuchs M, Cates ME (2002) Comparative simulation study of colloidal gels and glasses. *Phys Rev Lett* 88:098301.
8. Foffi G, et al. (2002) Evidence for an unusual dynamical-arrest scenario in short-ranged colloidal systems. *Phys Rev E* 65:050802.
9. Zaccarelli E, et al. (2002) Confirmation of anomalous dynamical arrest in attractive colloids: A molecular dynamics study. *Phys Rev E* 66:041402.
10. Puertas AM, Fuchs M, Cates ME (2003) Simulation study of nonergodicity transitions: Gelation in colloidal systems with short-range attractions. *Phys Rev E* 67:031406.
11. Bergenholtz J, Poon WCK, Fuchs M (2003) Gelation in model colloid–polymer mixtures. *Langmuir* 19:4493–4503.
12. Pham KN, Egelhaaf SU, Pusey PN, Poon WCK (2004) Glasses in hard spheres with short-range attraction. *Phys Rev E* 69:011503.
13. van Megen W, Underwood SM (1994) Glass transition in colloidal hard spheres: Measurement and mode-coupling-theory analysis of the coherent intermediate scattering function. *Phys Rev E* 49:4206–4220.
14. van Megen W, Mortensen TC, Williams SR, Müller J (1998) Measurement of the self-intermediate scattering function of suspensions of hard spherical particles near the glass transition. *Phys Rev E* 58:6074–6085.
15. Zaccarelli E, Foffi G, Sciortino F, Tartaglia P (2003) Activated bond-breaking processes preempt the observation of a sharp glass–glass transition in dense short-ranged attractive colloids. *Phys Rev Lett* 91:108301.
16. Zaccarelli E, Sciortino F, Tartaglia P (2004) Numerical study of the glass–glass transition in short-ranged attractive colloids. *J Phys Condens Matter* 16:S4849–S4860.
17. Zaccarelli E (2007) Colloidal gels: Equilibrium and non-equilibrium routes. *J Phys Condens Matter* 19:323101.
18. Bergenholtz J, Fuchs M (1999) Gel transitions in colloidal suspensions. *J Phys Condens Matter* 11:10171–10182.
19. Bergenholtz J, Fuchs M, Voigtmann T (2000) Colloidal gelation and non-ergodicity transitions. *J Phys Condens Matter* 12:6575–6583.
20. Haw MD, Poon WCK (1997) Mesoscopic structure formation in colloidal aggregation and gelation. *Adv Colloid Interface Sci* 73:71–126.

21. Lu PJ, et al. (2008) Gelation of particles with short-range attraction. *Nature* 453:499–504.
22. Pham KN, et al. (2006) Yielding of colloidal glasses. *Europhys Lett* 75:624–630.
23. Pham KN, et al. (2006) Yielding behavior of repulsion- and attraction-dominated colloidal glasses. *J Rheol* 52:649–676.
24. Sciortino F, Tartaglia P, Zaccarelli E (2003) Evidence of a higher-order singularity in dense short-ranged attractive colloids. *Phys Rev Lett* 91:268301.
25. Solomon MJ, Varadan P (2001) Dynamic structure of thermoreversible colloidal gels of adhesive spheres. *Phys Rev E* 63:051402.
26. Bouchaud J-P, Georges A (1990) Anomalous diffusion in disordered media: Statistical mechanisms, models and physical applications. *Phys Rep* 195:127–293.
27. Weeks ER, Swinney HL (1998) Anomalous diffusion resulting from strongly asymmetric random walks. *Phys Rev E* 57:4915–4920.
28. Wei QH, Bechinger C, Leiderer P (2000) Single-file diffusion of colloids in one-dimensional channels. *Science* 287:625–627.
29. Weeks ER, Weitz DA (2002) Subdiffusion and the cage effect studied near the colloidal glass transition. *Chem Phys* 284:361–367.
30. Sperl M (2004) Dynamics in colloidal liquids near a crossing of glass- and gel-transition lines. *Phys Rev E* 69:011401.
31. Puertas A, Fuchs M, Cates ME (2007) Aging in attraction-driven colloidal glasses. *Phys Rev E* 75:031401.
32. Götze W (1991) in *Liquids, Freezing and Glass Transition*, eds Hansen J-P, Levesque D, Zinn Justin J (Elsevier, Amsterdam), p 287.
33. Götze W, Sperl M (2003) Logarithmic relaxation in glass-forming systems. *Phys Rev E* 66:011405.
34. Jenkins MC, Egelhaaf SU (2008) Confocal microscopy of colloidal particles: Towards reliable, optimum coordinates. *Adv Colloid Interface Sci* 136:65–92.
35. Besseling R, Isa L, Weeks ER, Poon WCK (2009) Quantitative imaging of colloidal flows. *Adv Colloid Interface Sci* 146:1–17.
36. Viehman DC, Schweizer KS (2008) Cooperative activated dynamics in dense mixtures of hard and sticky spheres. *Phys Rev E* 78:051404.
37. Kob W, Barrat J-L (1997) Aging effects in a Lennard–Jones glass. *Phys Rev Lett* 78:4581–4584.